Available online at www.sciencedirect.com
ScienceDirect
Trans. Nonferrous Met. Soc. China 26(2016) 895−904
Transactions of Nonferrous Metals Society of China
www.tnmsc.cn

Characteristics evolution of 6009/7050 bimetal slab prepared by direct-chill casting process

Guang-yuan YAN[1], Feng MAO[1], Fei CHEN[1], Wei WU[1], Zhi-qiang CAO[2], Tong-min WANG[1], Ting-ju LI[2]

1. Key Laboratory of Materials Modification by Laser, Ion, and Electron Beams, Ministry of Education, School of Materials Science and Engineering, Dalian University of Technology, Dalian 116024, China;
2. Laboratory of Special Processing of Raw Materials, Dalian University of Technology, Dalian 116024, China

Received 18 May 2015; accepted 10 October 2015

Abstract: 6009/7050 alloy bimetal slab was prepared by a direct-chill (DC) casting process. Homogenizing annealing, hot rolling and T6 treatment were successively performed and their effects on microstructure and properties of the slab were studied. The results reveal that the average diffusion layer thickness of as-cast slab, determined by interdiffusion of elements Zn, Cu, Mg and Si, was about 400 μm. Excellent metallurgical bonding was achieved because all tensile samples fractured on the softer 6009 alloy side after homogenizing annealing. After homogenizing annealing plus rolling, the average diffusion layer thickness decreased to 100 μm, while the network structure of 7050 alloy side transformed to dispersive nubby structure. Furthermore, subsequent T6 treatment resulted in diffusion layer thickness up to 200 μm and an obvious increase of the Vickers hardness for both 7050 and 6009 sides. The layered structure of the as-cast 6009/7050 bimetal is retained after hot rolling and T6 treatment.

Key words: 7050 alloy; bimetal slab; direct-chill casting; heat treatment; hot rolling

1 Introduction

Bimetallic materials have been widely used in many industrial fields due to the combination of excellent physical and chemical properties of the base metals, which cannot be achieved by the individual alloy acting alone [1]. Several conventional approaches have been used to manufacture the bimetallic materials including rolling bonding [2−5], explosive welding [6−9], diffusion bonding [10−13], extrusion cladding [14,15], centrifugal casting [16], laser cladding [17], and so on. LI et al [18] prepared 7075/6009 aluminum composite ingot by double-stream-pouring continuous casting. Compared with these methods, direct-chill (DC) casting provides many advantages, such as lower cost, superior metallurgical bonding and high productivity, and has been applied to prepare lots of industrial used bimetals. WAGSTAFF et al [19] investigated the clad ingot produced by the well-known Novelis fusion process. SUN et al [20] produced Al−Si alloy and Al−Mn alloy bimetal slab using continuous casting. FU et al [21] illustrated the microstructure and mechanical properties of Al−1Mn and Al−10Si alloy circular clad ingot prepared by DC casting. LIU et al [22] produced the 3003/4045 clad hollow billet via horizontal continuous casting. WANG et al [23] investigated the development of Al−Li and Al−Mn bimetal slab prepared by a modified DC casting process. However, up to date, few literatures exist reporting on the successful using DC casting to produce bimetals containing Al−Zn−Mg−Cu high-strength alloys, which can be used widely in aerospace field.

The 7050 alloy, typical Al−Zn−Mg−Cu high-strength alloy, is considered as an ideal material for preparing aircraft skin due to its high specific strength [24]. However, it suffers from the poor corrosion resistance and is prone to cracking during solidification and rolling process. The 6009 alloy has superior corrosion resistance and good formability, and is widely applied in automobile plates, but its applications limited in the low strength [25]. The 6009/7050 bimetal material combines the advantages of two alloys and features high strength and superior corrosion resistance as well as good formability, which could meet the requirements of mass reduction and safety improvement

Foundation item: Project (51375070) supported by the National Natural Science Foundation of China
Corresponding author: Zhi-qiang CAO; Tel: +86-411-84706169; Fax: +86-411-84706169; E-mail: caozq@dlut.edu.cn
DOI: 10.1016/S1003-6326(16)64184-5

in automobile and airplane industries.

In this work, a 6009/7050 bimetal slab was prepared by a DC casting process. The fabricated slabs were subjected to homogenizing annealing, hot rolling, solid solution and aging. The microstructure, composition distribution and mechanical properties of the as cast, rolled and heat treated slab were studied in detail.

2 Experimental

2.1 Materials and ingot preparation

The chemical compositions of the 6009 and 7050 alloy are given in Table 1. The schematic diagram of experimental setup is shown in Fig. 1. Three dominant factors influencing the metallurgical bonding between two alloys are pouring temperature, elevating speed and cooling water flow rate. As presented in Fig. 1, the hot top was fixed on the top of a mold. The water-cooled baffle was placed into the mold as inner mold and the cooling water flow can be controlled. A layer of refractory material to insulate the heat covered on one side of the water-cooled baffle and the water passage was embedded on the other side. The 6009 alloy melt at 670 °C was firstly poured into the left part of the mold and a semisolid shell would be formed once the melt contacted with the water cooled side of water cooled dividing baffle. The 7050 melt at 730 °C was then poured into the right part of the mold when the 6009 semisolid shell was strength enough, at the same time, the dividing baffle was drawn up to keep the relative motion between the bimetal slab and the water-cooled baffle at the speed of 60 mm/min, and the cooling water flow rate is 140 L/h. After the baffle and melts were separated, the bimetal ingot (130 mm × 120 mm × 100 mm) was fabricated successfully. After a series of systematic experiments, the optimized experimental parameters were as follows: the pouring temperatures were 730 °C and 670 °C for 7050 and 6009 alloys, respectively; the drawing speed of the dividing baffle was 60 mm/min, and the cooling water flow rate was 140 L/h.

Table 1 Chemical compositions of experimental alloys (mass fraction, %)

Alloy	Zn	Cu	Mg	Si
7050	6.5327	2.2728	2.2852	0.0557
6009	−	−	0.6032	0.9547
Alloy	**Fe**	**Mn**	**Cr**	**Al**
7050	0.1090	0.0026	0.0256	Bal.
6009	0.1307	0.0034	0.0209	Bal.

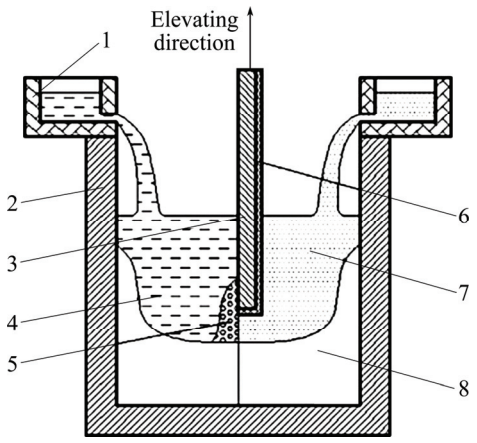

Fig. 1 Schematic illustration of modified direct-chill casting process: 1—Hot top; 2—Mold; 3—Water cooled baffle; 4—6009 alloy melt; 5—6009 alloy semisolid shell; 6—Heat insulation layer; 7—7050 alloy melt; 8—Bimetal slab

2.2 Homogenizing annealing, rolling, solid solution and aging

As presented in Fig. 2, the test sample was prepared with a length of 100 mm, width of 15 mm and thickness of 15 mm by wire-electrode cutting technique from the bimetal slab (130 mm × 120 mm × 100 mm).

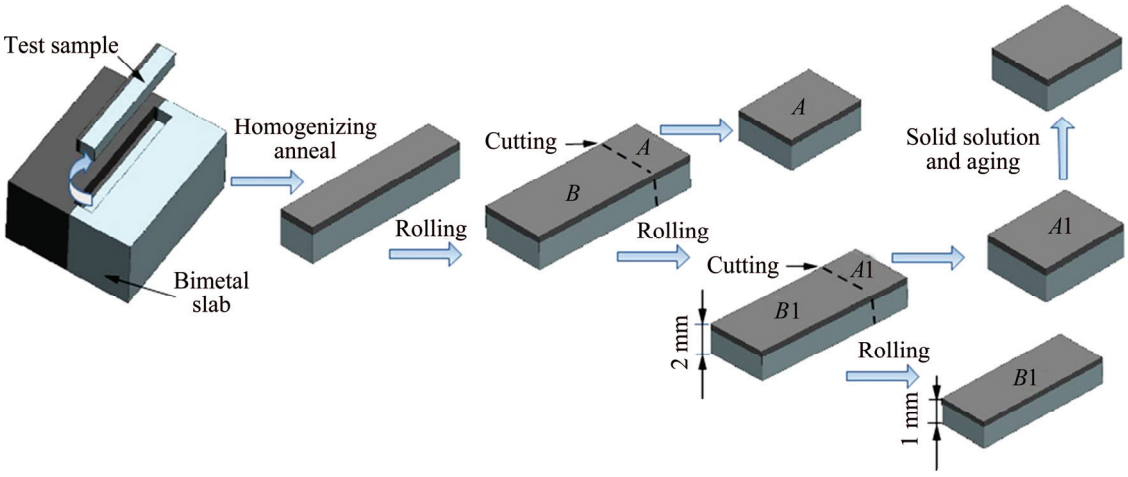

Fig. 2 Schematic illustration of heat treatment and plastic deformation procedures of bimetal sample

Homogenizing annealing was firstly performed on test sample at 460 °C for 24 h and then cooled inside the furnace to room temperature. After homogenizing annealing, the test sample with 15 mm in thickness was rolled at (450±5) °C to produce a 6 mm thick plate. The 6 mm thick plate was then cut into two parts (part A and part B) along the dashed line shown in Fig. 2. Part A (the smaller part) was used as the specimen for microstructure observation, composition distribution analysis and hardness measurement, while part B (the larger part) continued to be rolled into 4 mm thick plate under the same rolling conditions. This process was sequentially repeated to produce 2 mm and 1 mm thick plates. Four test plates were thus acquired after rolling processes. Solution treatment was performed on the 2 mm thick plate after homogenizing annealing and rolling at 475 °C for 40 min, followed by water-immersion quenching with a maximum delay of 6 s. Shortly thereafter, the 2 mm thick plate was subjected to an artificial aging treatment at 175 °C for 10 h.

2.3 Structure observation, composition analysis and properties test

The macrostructure image is obtained after milling. The as-cast, homogenizing annealed, hot rolled, and T6 treated specimens were polished and etched with Keller's reagent (1% HF+1.5% HCl+2.5% HNO_3+95% distilled water), then observed by optical microscope and scanning electron microscope (SEM) equipped with energy dispersive spectrometer (EDS). Electron microprobe (EPMA) was applied to reveal the alloy elements composition in the interfacial region of the bimetal samples. Tensile tests were performed using a DNS 100 test machine with a strain rate of 2 mm/min. The Vickers hardness variation in the interfacial region of the test samples was measured with a load of 50 g for 15 s.

3 Results and discussion

3.1 Microstructure and composition analysis

Figure 3 shows the macrostructure and microstructure of the 6009/7050 bimetal slab. The 6009 and 7050 materials are distinctly separated, and the interface is clearly identified due to the brightness contrast between the alloys after fine milling (Fig. 3(a)). The straight interface is obtained without any inclusions and porosities. Figure 3(b) shows the microstructure of the bimetal slab at the interface. On the 7050 alloy side, the network structure distributes at the grain boundary. On the 6009 alloy side, no apparent precipitated phases can be seen at the grain boundary. In addition, there are no discontinuities at the interface, indicating that a good metallurgical bonding between the two alloys is achieved.

Figure 4 clearly shows two main precipitated phases

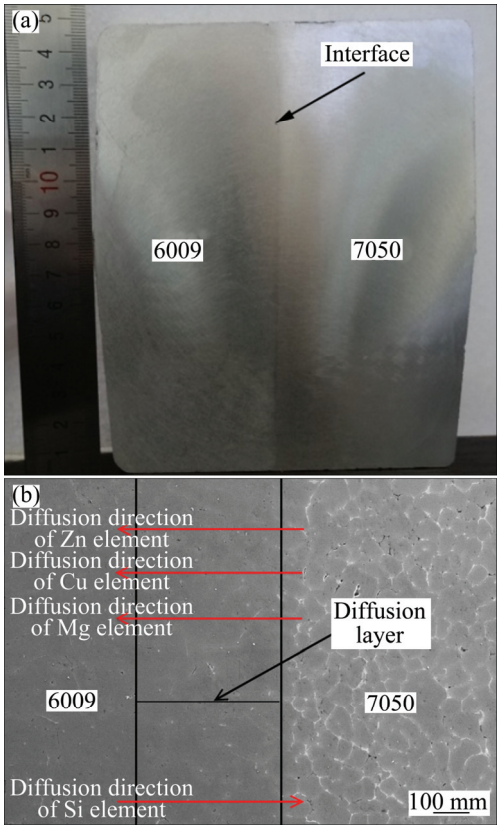

Fig. 3 Cross sectional image (a) and interface microstructure (b) of as-cast bimetal slab

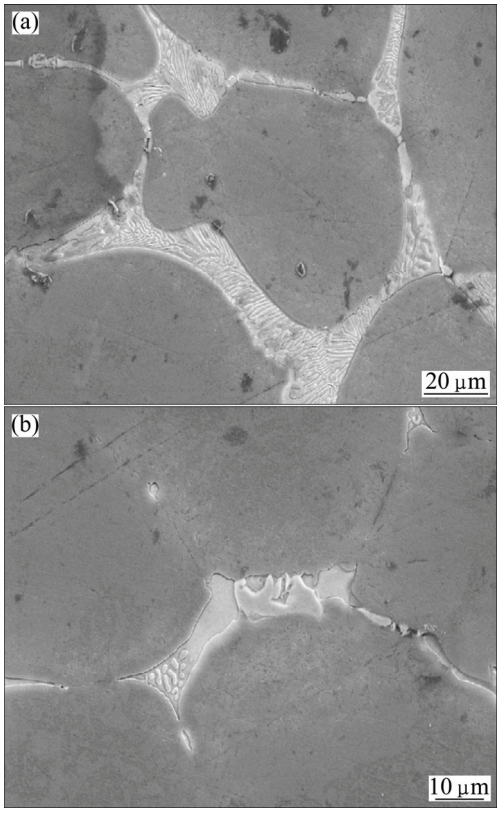

Fig. 4 SEM images of network structure (a) and plate-like phase (b) distributed at grain boundary on 7050 alloy side

distributed at the grain boundary on the 7050 alloy side. As can be seen, the network structure principally consists of skeletal structure (Fig. 4(a)) and the plate-like phases (Fig. 4(b)). According to the EPMA results, the composition of skeletal eutectic structure is 23.467% Zn, 24.856% Cu, 13.450% Mg and 38.127% Al (mass fraction), which is in accordance with the α(Al) + T(AlZnMgCu) eutectic structure. The eutectic phase is also considered to be $T(Al_2Mg_3Zn_3)$ + $S(Al_2CuMg)$ [26]. The composition of the plate-like phase is 31.067% Cu and 45.379% Al, which is close to Al_2Cu phase in composition.

The layer of semisolid shell formed when 6009 melt contacted the water-cooled baffle. This shell would served as a heterogeneous nucleation substrate for the primary α(Al) phase of the 7050 alloy. Once the 7050 melt was poured into the mould, α(Al) started to nucleate and grew on the surface of 6009 semisolid shell.

Moreover, the 7050 alloy is enriched with Zn, Cu, Mg elements, while the 6009 primarily contains Mg and Si elements. As concentration difference of these elements exists between the two alloys, according to Fick's Law, interdiffusion takes place in the vicinity of the interface, i.e., Zn, Cu and Mg atoms diffuse from the 7050 side to the 6009 side, while Si atoms move in an opposite direction during solidification. This implies that solute distribution in the diffusion layer is important.

Figure 5 shows the composition variations of the Zn, Cu, Mg and Si elements in the diffusion layer. Three parts can be seen: the 7050 alloy in right side, diffusion layer in the middle and the 6009 alloy in left hand. From 7050 to diffusion layer, the contents of Zn, Cu and Mg elements tend to decrease rapidly, and the same case is found from diffusion layer to 6009 alloy side, while the contents of these elements decrease gradually across the diffusion layer. This finding is consistent with the foregoing inference that 6009 serves as a heterogeneous nucleation substrate for the primary α(Al) of the 7050 alloy. In present study, the thickness of diffusion layer, defined as the diffusion distance of Zn element across the interface, is found to be 400 μm.

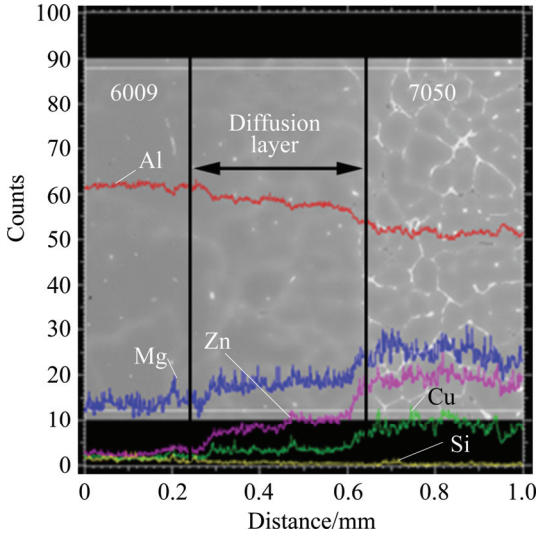

Fig. 5 EPMA line analysis of as-cast bimetal slab

3.2 Mechanical properties

The variation of Vickers hardness across the interface of the bimetal is presented in Fig. 6. The average hardness in the 7050 side was about HV 125 while that in the 6009 side, was about HV 60. The hardness of the interfacial region tended to decrease gradually from 7050 alloy side to 6009 alloy side, namely, the hardness of the interface was higher than that of 6009 alloy and lower than that of 7050 alloy. In addition, the Vickers hardness (HV) and yield strength (σ) of the material approximately obey the three times relationship, i.e. HV≈3σ [27]. Thus, it can be concluded that the yield strength of interface is also higher than that of 6009 alloy and lower than that of 7050 alloy, which can be attributed to the effect of solution strengthening by diffused atoms.

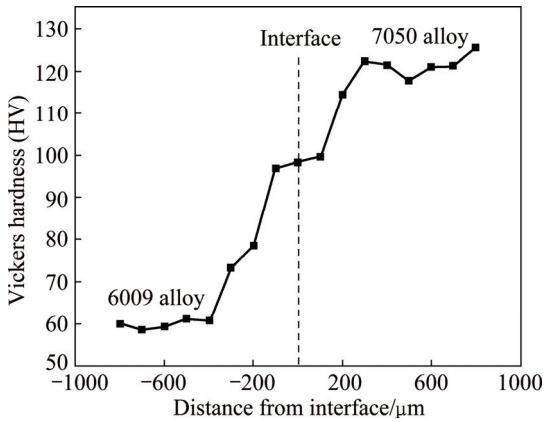

Fig. 6 Vickers hardness distribution across bonding interface of as-cast bimetal slab

Bonding strength of the bimetal slab is measured by performing tensile test. The schematic illustration of the tensile specimen is presented in Fig. 7(a). Figure 7(b) shows the homogenizing-anneal sample after tensile test. The tensile fractures of all the homogenizing-annealed simples occurred on the lower strength 6009 alloy side, while the interface remained well. The results are consistent with the report that the plasticity predominantly occurs in the softer component of the compound tensile samples, and failure occurs when the ultimate tensile strength of the softer component is reached [28]. Figure 8 shows the tensile strength−displacement curves of the tensile sample. The tensile strength of the homogenizing-annealed bimetal clad was about 100 MPa, which was close to the strength of the 6009 alloy. Thus, the tensile strength of interface was higher than that of 6009, suggesting an excellent

metallurgical bonding between the 7050 alloy and 6009 alloy.

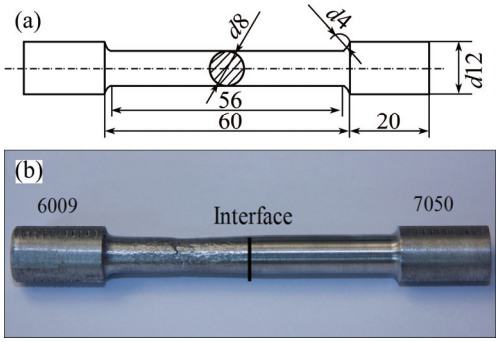

Fig. 7 Schematic illustration of tensile specimen (a) and tensile fractured sample (b) (unit: mm)

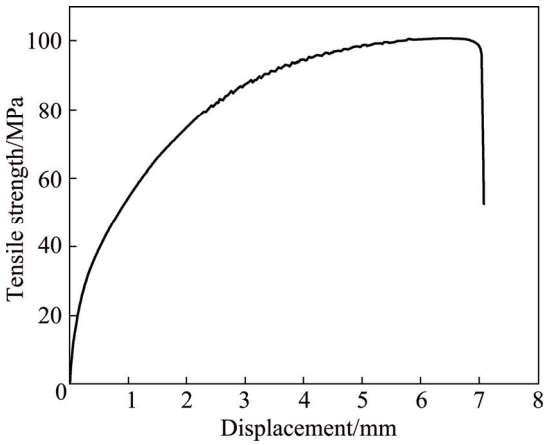

Fig. 8 Tensile strength−displacement curves of homogenizing annealing sample

3.3 Homogenizing annealing and plastic deformation

It is essential to perform homogenizing annealing on the as-cast bimetal slab before rolling since homogenizing annealing decreases resistance to plastic flow of 7050 alloy, and reduces the content of bulky precipitated phases distributed at grain boundaries of 7050 alloy to avoid crazing during rolling.

The variation of the clad ratio and the thickness of 6009 during hot rolling is presented Fig. 9. Clad ratio is defined as the ratio of the 6009 thickness to the total sample thickness. When the plate was rolled from 15 to 4 mm, the clad ratio was stable at around 20%. As the rolling temperature was 450 °C, the resistance to plastic flow of 7050 alloy declined so much compared to as-cast alloy that it was close to the resistance to plastic flow of 6009 alloy, and this gave rise to the compatible deformation during rolling. Further rolling to 1 mm plate, the clad ratio increased from 20% to 23%. This slight improvement of clad ratio can be attributed to the less increment in the plastic flow resistance of 7050 alloy than that of 6009 alloy.

Figure 10 shows the microstructure of homogenizing-annealed 6009/7050 clad samples after rolling to different thicknesses along the deformation direction. The two layers in as-cast state were still maintained after rolling process. When the sample was rolled to 6.14 mm plate (Fig. 10(a)), the net structure of 7050 side began to fade away, most of the coarse (α(Al) + T(AlZnMgCu)) eutectic structure fragmented and part of them was dissolved. Besides, it is clear to see plastic deformation near the interfacial region on 7050 side. With the further reduction of the simple thickness, the eutectic structure transformed to dispersive nubby phase, and the net structure of 7050 side disappeared completely. In addition, as is shown in Figs. 10(b)−(d), the fine and dispersive phases can be seen obviously in the matrix on both 6009 and 7050 alloy sides.

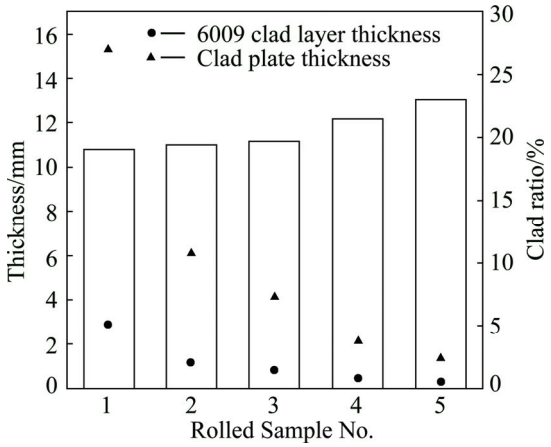

Fig. 9 Variation of clad ratio and 6009 clad layer thickness in bimetal after homogenizing annealing and rolling process (Sample 1: 15.32 mm; Sample 2: 6.14 mm; Sample 3: 4.14 mm; Sample 4: 2.15 mm; Sample 5: 1.35 mm)

The content variations of the Zn, Cu, Mg and Si elements across the interface of the rolled 2.15 mm bimetal slab are presented in Fig. 11. Compared to the as-cast sample (Fig. 5), the thickness of diffusion layer decreased to about 100 μm after homogenizing annealing and rolling, indicating that the decrement in the thickness of diffusion layer caused by plastic deformation is larger than the increment caused by atoms diffusion during the rolling and annealing.

Figure 12 shows the distribution of Zn, Cu, Mg and Si elements at the interface. The result reveals that, despite that it has been rolled to 2.15 mm, bimetal slab retains the layered characteristics of as-cast, a distinct boundary can be seen and there is a big difference in the contents of Zn and Mg elements between 7050 alloy and 6009 alloy. Due to dissolution and fragment of (α(Al) + T(AlZnMgCu)) eutectic structure, the dispersive nubby phases can be seen on 7050 alloy side. These dispersive nubby phases are enriched with Cu and Mg elements instead of Zn element. Nonuniform Cu is due to its larger radius, which causes more difficult diffusion compared

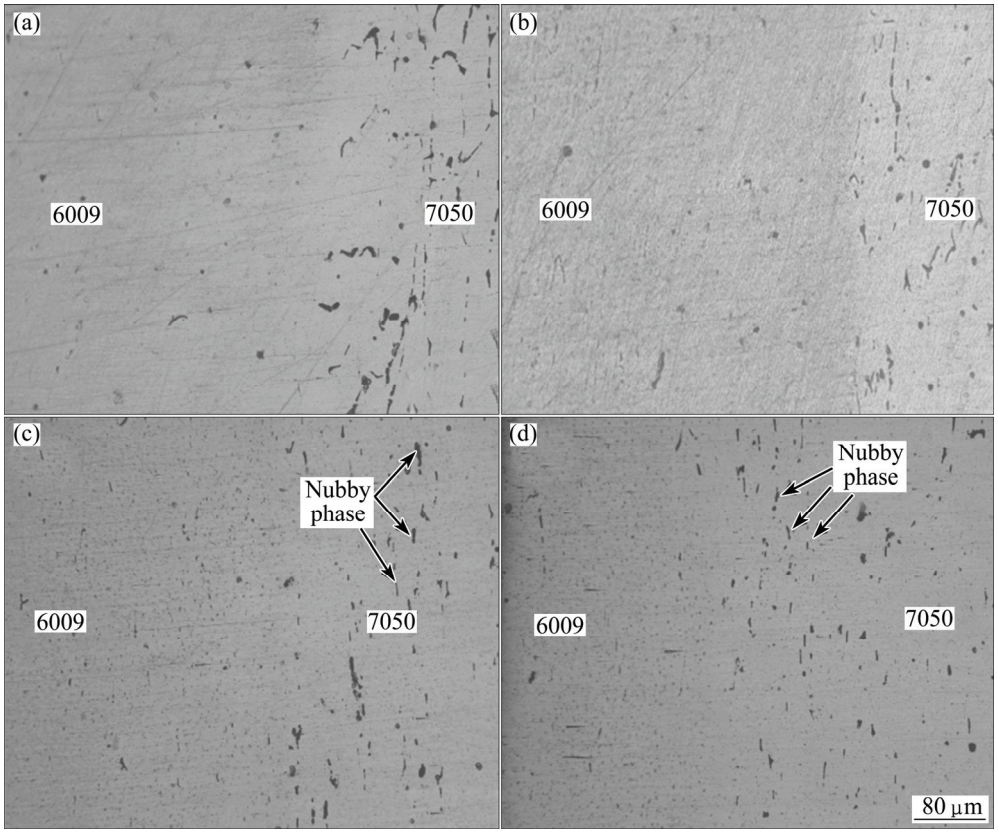

Fig. 10 Microstructures of interfacial region of homogenizing-annealed clad samples after rolling: (a) 6.14 mm; (b) 4.14 mm; (c) 2.15 mm; (d) 1.35 mm

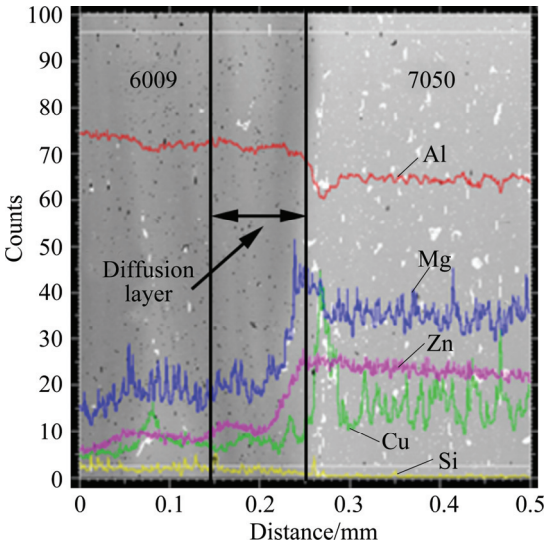

Fig. 11 EPMA line analysis of 2.15 mm homogenizing-annealed bimetal slab after rolling

to Mg and Zn. A small quantity of Mg element is enriched in the residual phase because the diffusion time is not enough for Mg element to diffuse into α(Al) matrix completely. With the faster diffusion speed, the distribution of Zn element is more uniform compared to Mg and Cu elements.

Variation of microhardness across the interface of the homogenizing-annealed sample after rolling is shown in Fig. 13. The result reveals that the layered characteristics of the microhardness distribution were retained. When the annealed sample was rolled to 6.14 mm, the average hardness of 7050 alloy side was about HV 110, while that of the 6009 alloy side was about HV 45. Further rolling to 1.35 mm (Figs. 13(a)−(c)), the microhardnesses of the 7050 alloy and 6009 sides increased to about HV 132 and HV 62, respectively. This further increased hardness was attributed to work hardening behavior and precipitation strengthening mechanism.

3.4 T6 treatment

Solid solution and aging were performed on the 2.15 mm sample after homogenizing annealing and rolling. The backscattered micrograph in the interfacial region and the composition variation of Zn, Cu, Mg and Si elements and are shown in Fig. 14. Compared to element distribution of rolled sample (Fig. 11), it can be seen obviously that, the distance of diffusion layer increased from 100 μm to 200 μm due to solute atoms diffusion across the interface during solution treatment. The aforementioned fine and dispersive phases in rolled 7050 alloy dissolved into the matrix during solution treatment. Zn, Cu, Mg and Si elements diffused into

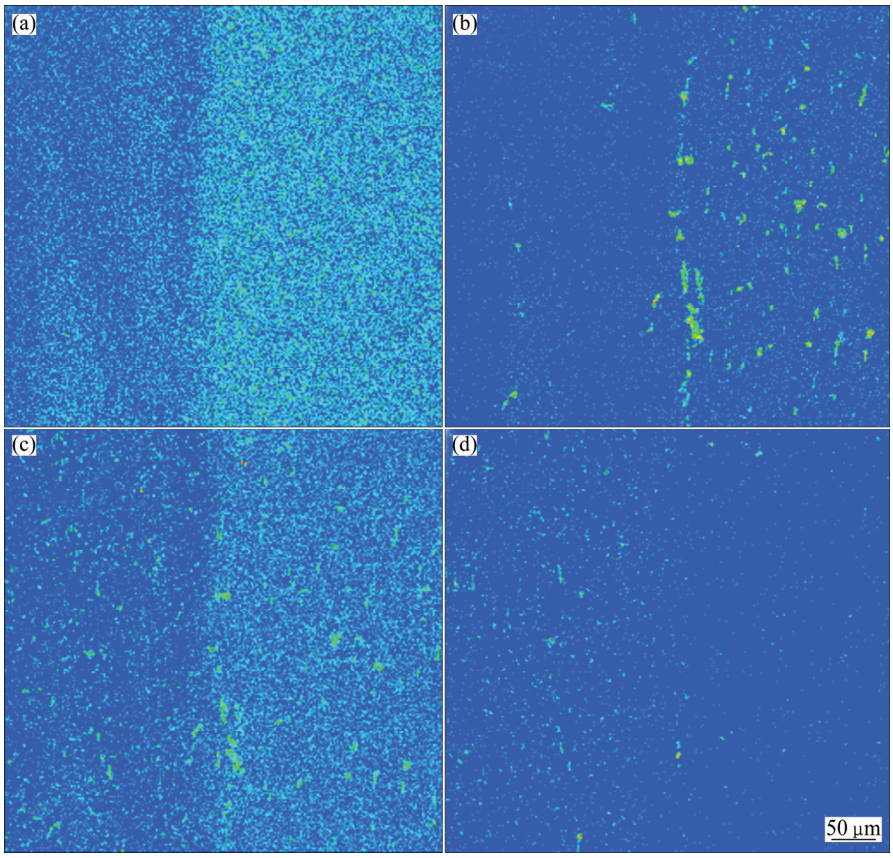

Fig. 12 EPMA analysis of 2.15 mm homogenizing-annealed sample after rolling element mapping of Zn (a), Cu (b), Mg (c) and Si (d) in interfacial region

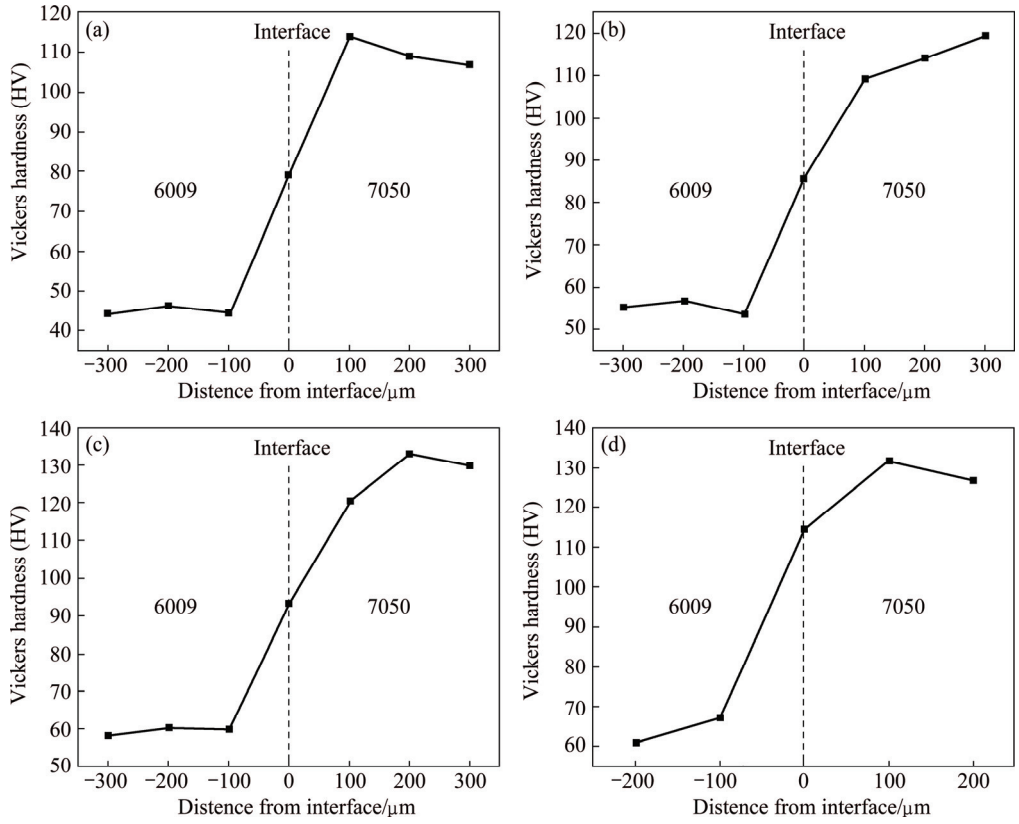

Fig. 13 Microhardness distribution across interfacial region of homogenizing-annealed samples after rolling: (a) 6.14 mm; (b) 4.14 mm; (c) 2.15 mm; (d) 1.35 mm

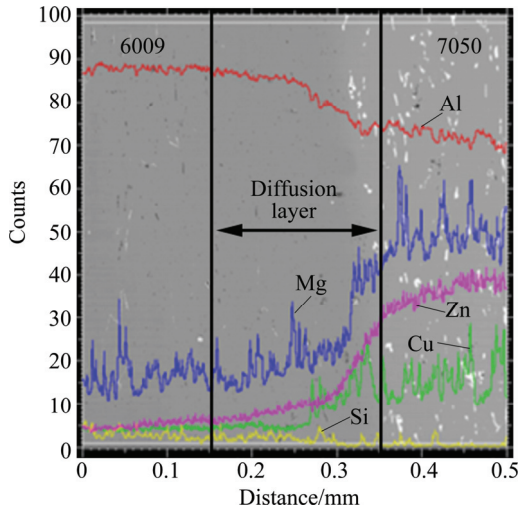

Fig. 14 Distribution of Zn, Cu, Mg and Si elements and backscattered micrograph in interfacial region of rolled 2.15 mm bimetal slab after T6 heat treatment

α(Al) matrix during solution treatment, which lead to the redistribution of these element after aging. Figure 15 shows the element mapping of Zn, Cu, Mg and Si elements of the 2.15 mm thick bimetal slab after homogenizing-anneal, rolling and T6 treatment. The result reveals that composition distribution of the bimetal slab still maintains layered characteristics of as-cast state. Compared to rolled state (Fig. 11), the Mg and Zn elements distribution of the sample after T6 treatment on 7050 alloy side is more uniform due to atoms diffusion during solution and aging, while Cu element still gathers in the residual nubby phase due to its poor diffusion ability. On the 6009 alloy side, the massive precipitate phases are enriched with Cu and Si elements.

Figure 16 shows the Vickers hardness variation across the interfacial region of the sample after homogenizing annealing, rolling and T6 heat treatment. It can be seen that the average microhardness values of both 7050 and 6009 alloy sides show an obvious increase compared to the condition after homogenizing annealing and rolling. The hardness of the 7050 side was about HV 172, and about HV 80 for 6009 alloy after T6 heat treatment. The promoted hardness was attributed to precipitation strengthening and solid solution strengthening mechanisms. RANGANATHA et al [29] reported that the presence of fine precipitate structure of GP zones and metastable phase $\eta(MgZn_2)$ was attributed to the strengthening of AA7049 alloy after T6 heat treatment.

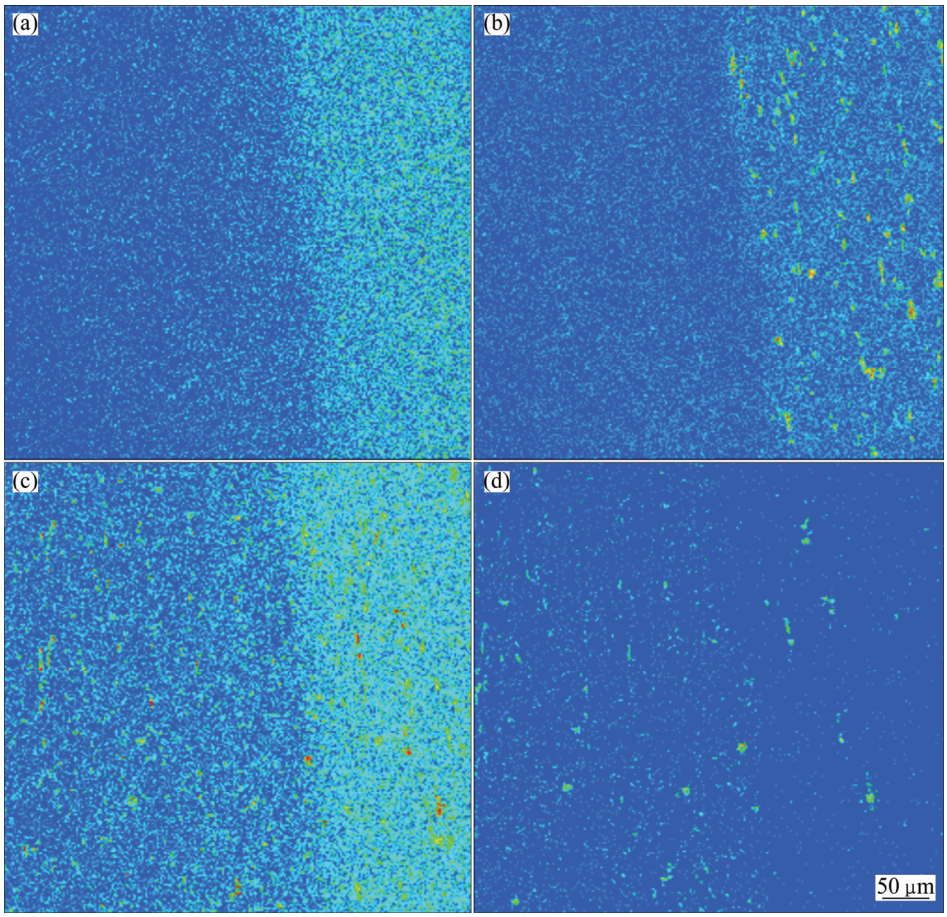

Fig. 15 Element mappings of Zn (a), Cu (b), Mg (c) and Si (d) in interfacial region of rolled 2.15 mm bimetal slab after T6 heat treatment

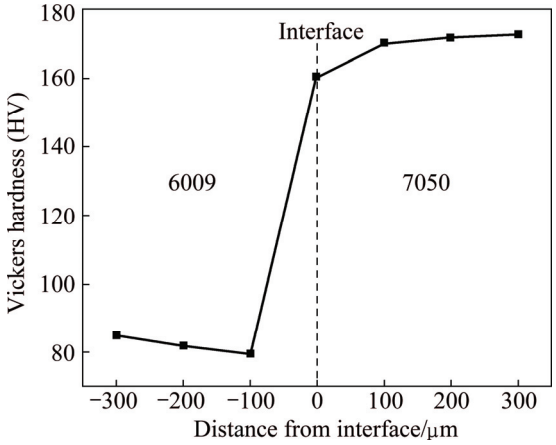

Fig. 16 Vickers hardness distribution across bonding interface of rolled 2.15 mm bimetal slab after T6 heat treatment

4 Conclusions

1) 6009/7050 bimetal could be successfully prepared by a direct-chill casting process with optimized experimental parameters.

2) The earlier poured 6009 alloy melt served as the heterogeneous nucleation substrate for the 7050 alloy. Interdiffusion of Zn, Cu, Mg and Si elements took place in the interfacial region, which resulted in a 400 μm thick diffusion layer.

3) The tensile strength of the bimetal after homogenizing annealing averaged at 100 MPa. The fracture located on the softer 6009 side, which indicated an excellent metallurgical bonding between 6009 alloy and 7050 alloy.

4) After hot rolling, the network structure of 7050 alloy side transformed into dispersive nubby phase and the thickness of the diffusion layer was decreased to 100 μm. The Vickers hardness of 7050 alloy, interface and 6009 alloy are all increased upon hot rolling.

5) The interface can be strengthened and the diffusion layer thickness was increased to 200 μm after subsequent T6 treatment.

References

[1] KIM J K, YU T X. Forming and failure behaviour of coated, laminated and sandwiched sheet metals: A review [J]. Journal of Materials Processing Technology, 1997, 63: 33−42.

[2] KANG H G, KIM J K, HUH M Y, ENGLAR O. A combine texture and FEM study of strain states during rolling-clading of five stainless steel/aluminum composites [J]. Materials Science and Engineering A, 2007, 452−453: 347−358.

[3] KIM S H, KIM H W, EUH K, KANG J H, CHO J H. Effect of wire brushing on warm roll bonding of 6xxx/5xxx/6xxx aluminum alloy clad sheets [J]. Materials and Design, 2012, 35: 290−295.

[4] ZHANG X P, CASTAGNE S, YANG T H, GU C F, WANG J T. Entrance analysis of 7075 Al/Mg−Gd−Y−Zr/7075 Al laminated composite prepared by hot rolling and its mechanical properties [J]. Materials and Design, 2012, 32: 1152−1158.

[5] CHANG H, ZHENG M Y, GAN W M, WU K, MAAWAD E, BROKMEIER H G. Texture evolution of the Mg/Al laminated composite fabricated by the accumulative roll bonding [J]. Scripta Materialia, 2009, 61: 717−720.

[6] AKBARI-MOUSAVI S A A, BATTETT L M, AL-HASSANI S T S. Explosive welding of metal plates [J]. Journal of Materials Processing Technology, 2008, 202: 224−239.

[7] YAN Y B, ZHANG Z W, SHEN W, WANG J H, ZHANG L K, CHIN B A. Microstructure and properties of magnesium AZ31−aluminum 7075 explosively welded composite plate [J]. Materials Science and Engineering A, 2010, 527: 2241−2245.

[8] FEHIM F. Recent developments in explosive welding [J]. Materials and Design, 2011, 32: 1081−1093.

[9] BEHCET G. Investigation of interface properties and weldability of aluminum and copper plates by explosive welding method [J]. Materials and Design, 2008, 29: 275−278.

[10] JINDRICH Z, SHUNSUKE H, HIROAKI O. Diffision bondability of similar/dissimilar light metal sheets [J]. Journal of Materials Processing Technology, 2007, 186: 87−93.

[11] WANG De-qing, SHI Zi-yuan, QI Ruo-bin. Cladding of stainless steel on aluminum and carbon steel by interlayer diffusion bonding [J]. Scripta Materialia, 2007, 56: 369−372.

[12] WANG Juan, LI Ya-jiang, LIU Peng, GENG Hao-ran. Microstructure and XRD analysis in the interface zone of Mg/Al diffusion bonding [J]. Journal of Materials Processing Technology, 2008, 205: 146−150.

[13] LIU L M, ZHAO L M, XU R Z. Effect of interlayer composition on the microstructure and strength of diffusion bonded Mg/Al joint [J]. Materials and Design, 2009, 30: 4548−4551.

[14] LEE J S, SON H T, OH I H, KANG C S, YUN C H, LIM S C, WON H C K. Fabrication and characterization of Ti−Cu clad materials by indirect extrusion [J]. Journal of Materials Processing Technology, 2007, 187−188: 653−656.

[15] LIU X B, CHEN R S, HAN E H. Preliminary investigations on the Mg-Al-Zn/Al laminated composite fabricated by equal channel angular extrusion [J]. Journal of Materials Processing Technology, 2009, 209: 4675−4681.

[16] WANG Kai, XUE Han-song, ZOU Mao-hua, LIU Chang-ming. Microstructural characteristics and properties in centrifugal casting of SiC_p/X1104 composite [J]. Transactions of Nonferrous Metals Society of China, 2009, 19(6): 1410−1415.

[17] SEXTON L, LAVIN S, BYRNE G, KENNEDY A. Laser cladding of aerospace materials [J]. Journal of Materials Processing Technology, 2002, 122: 63−68.

[18] LI Yuan-yuan, ZHENG Xiao-ping, ZHANG Wen-wen, LUO Zong-qiang. Effect of deformation temperature on microstructures and properties of 7075/6009 alloy [J]. Transactions of Nonferrous Metals Society of China, 2009, 19(5): 1037−1043.

[19] WAGSTAFF R B, LLOYD D J, BISCHOFF T F. Direct chill casting of clad ingot [J]. Materials Science Forum, 2006, 519−521: 1809−1814.

[20] SUN Jian-bo, SONG Xiao-yang, WANG Tong-min, YU Ying-shui, SUN Min, CAO Zhing-qiang, LI Ting-ju. The microstructure and property of Al−Si alloy and Al−Mn alloy bimetal prepared by comtinous casting [J]. Materials Letters, 2012, 67: 21−23.

[21] FU Ying, JIE Jin-chuan, WU Li, PARK J, SUN Jian-bo, KIM J, LI Ting-ju. Microstructure and mechanical properties of Al−1Mn and Al−10Si alloy circular clad ingot prepared by direct chill casting [J]. Materials Science and Engineering A, 2013, 561: 239−244.

[22] LIU Ning, JIE Jin-chuan, LU Yi-ping, WU Li, LI Ting-ju. Characteristics of clad aluminum hollow billet prepared by horizontal continuous casting [J]. Journal of Materials Processing Technology, 2014, 214: 60−66.

[23] WANG Tong-min, LIANG Chun-hui, CHEN Zong-ning, ZHENG Yuan-ping, KANG Hui-jun, WANG Wei. Development of an 8090/3003 bimetal slab using a modified direct-chill casting process [J]. Journal of Materials Processing Technology, 2014, 214: 1806−1811.

[24] ZOU Liang, PAN Qing-lin, HE Yun-bin, WANG Chang-zhen, LIANG Wen-jie. Effect of minor Sc and Zr addition on microstructures and mechanical properties of Al−Zn−Mg−Cu alloys [J]. Transactions of Nonferrous Metals Society of China, 2007, 17(2): 340−345.

[25] ZHONG H, ROMETSCH P, ESTRIN Y. Effect of alloy composition and heat treatment on mechanical performance of 6xxx aluminum alloys [J]. Transaction of Nonferrous Metals Society of China, 2014, 24(7): 2174−2178.

[26] CONG Fu-guan, ZHAO Gang, JIANG Feng, TIAN Ni, LI Rui-feng. Effect of homogenization treatment on microstructure and mechanical properties of DC cast 7X50 aluminum [J]. Transactions of Nonferrous Metals Society of China, 2015, 25(4): 1027−1034.

[27] ZHANG P, LI S X, ZHANG Z F. General relationship between strength and hardness [J]. Materials Science and Engineering A, 2011, 529: 62−73.

[28] LLOYD D J, GALLERNEAULT M, WAGSTAFF R B. The deformation of clad aluminum sheet produced by direct chill casting [J]. Metallurgical and materials transactions A: Physical Metallurgy and Material Science, 2010, 41: 2093−2103.

[29] RANGANATHA R, KUMAR V A, NANDI V S, BHAT R R, MURALIDHARA B K. Multi-stage heat treatment of aluminum alloy AA 7049 [J]. Transactions of Nonferrous Metals Society of China, 2013, 23(6): 1570−1575.

直接冷却法制备的 6009/7050 复层板坯的特征演化

闫光远[1]，毛 丰[1]，陈 飞[1]，吴 伟[1]，曹志强[2]，王同敏[1]，李廷举[2]

1. 大连理工大学 材料科学与工程学院 三束材料改性教育部重点实验室，大连 116024；
2. 大连理工大学 原材料特种制备技术实验室，大连 116024

摘 要：采用直接冷却铸造法制备 6009/7050 复层板坯。通过对该板坯先后进行均匀化退火、热轧和 T6 热处理，研究其对复层板坯组织和性能的影响。研究结果表明，铸态下该复层板坯的平均扩散层厚度约为 400 μm，扩散层厚度是由锌、铜、镁和硅的互扩散决定的。拉伸试验表明，复层板坯实现了良好的冶金复合，因为均匀化后的拉伸试样全部在较软的 6009 合金侧发生断裂。经过均匀化退火加热轧处理，平均扩散层厚度降低到 100 μm，同时 7050 合金侧的网状结构转变为分散的块状相。再经过 T6 热处理后，平均扩散层厚度增加为 200 μm，并且 7050 合金侧和 6009 合金侧的维式硬度均有明显地提高。经过热轧和 T6 热处理后，6009/7050 复层铸坯的层状结构被保留下来。

关键词：7050 合金；复层板坯；直接冷却铸造；热处理；热轧

(Edited by Yun-bin HE)